Available online at www.sciencedirect.com
ScienceDirect
Journal of Nuclear Materials 362 (2007) 459–465
journal of nuclear materials
www.elsevier.com/locate/jnucmat

Irradiation effects on thorium phosphate diphosphate: Chemical durability and thermodynamic study

C. Tamain [a], N. Dacheux [a,*], F. Garrido [b], L. Thomé [b]

[a] Groupe de Radiochimie, IPNO, Université Paris-Sud-11, 91406 Orsay, France
[b] CSNSM, CNRS-IN2P3, Université Paris-Sud-11, 91405 Orsay, France

Abstract

Since thorium phosphate diphosphate (β-TPD) can be considered as a potential host specific matrix for the long-term storage of actinides in the field of an underground repository, it is necessary to study the irradiation effects on the chemical durability of this material. In this aim, leaching tests were realized on pre-irradiated thorium–uranium phosphate diphosphate (β-TUPD) samples. The evolution of the normalized leaching showed that thorium often precipitates as a neoformed phosphate-based solid onto the surface of the leached samples while uranium (IV) is released in the leachate consequently to its oxidation into the uranyl form. The pre-irradiation accelerates the formation of the neoformed phase. On the contrary, the characterization of the neoformed phase through various techniques (EPMA, XRD, μ-Raman) showed that the pre-irradiation has no effect on the thermodynamics equilibria occurring onto the surface of the samples.

PACS: 81.20.Fw; 81.05.Kn; 82.60.Lf; 64.75.+g; 61.80.−x; 81.65.−b

1. Introduction

In the field of the long-term storage of nuclear waste, several phosphate ceramics were presented as good candidates for the immobilization of radionuclides including actinides. Among them, thorium phosphate diphosphate, β-$Th_4(PO_4)_4P_2O_7$ (β-TPD), appears as a good potential actinide-bearing phase, thanks to its high-capability of loading with large amounts of tetravalent actinides (up to 47.6 wt% in uranium) [1,2], its high-resistance to aqueous corrosion and its high-thermal stability [3]. However, due to the actinide loading, self-irradiation by α-decays could modify these initial performances, especially its chemical durability by increasing the chemical reactivity and modifying the thermodynamic stability of the material [4]. Consequently, it appeared necessary to study the consequences of irradiation on the dissolution of the material.

In this aim, sintered pellets were irradiated under ion beams of high-energy (840 MeV Kr ions) then submitted to leaching tests. These drastic conditions of irradiation were necessary to modify homogeneously the structure of the sample on the whole thickness which was altered during the leaching tests. It also enabled to study the behaviour of the ceramics in extreme conditions. The structural modifications under irradiation were quantified by

* Corresponding author. Tel.: +33 1 69 15 73 46; fax: +33 1 69 15 71 50.
E-mail address: dacheux@ipno.in2p3.fr (N. Dacheux).

0022-3115/$ - see front matter © 2007 Elsevier B.V. All rights reserved.
doi:10.1016/j.jnucmat.2007.01.098

the amorphous fraction f_A, determined by XRD analyses [5]. It appeared that β-TPD could be fully, partly or un-amorphized (corresponding to amorphous fractions of $f_A = 1$, $0 < f_A < 1$ or $f_A = 0$, respectively), depending on the local energy loss and the fluence of irradiation.

The leaching tests were preferentially driven on pre-irradiated β-TUPD solid solutions β-$U_{0.4}Th_{3.6}(PO_4)_4P_2O_7$. Indeed, the substitution of thorium by uranium (IV) does not modify the structural properties of the ceramic and makes the determination of dissolution kinetics possible by using uranium as a tracer. Indeed, contrarily to thorium which quickly precipitates with phosphate anions as neoformed phases, uranium (IV) is oxidized into uranium (VI) which remains in solution [6]. Moreover, as β-TPD and β-TUPD present the same behaviour under irradiation, it was possible to simulate the β-TPD alteration in solution towards that of β-TUPD.

The kinetics aspect of the influence of the pre-irradiation was the aim of a first paper [7]. This study evidenced the significant influence of the amorphous fraction of pre-irradiated samples on the normalized dissolution rate, R_L, which is increased by a factor of 10–100 between unirradiated and fully amorphized materials. On the contrary, the pre-irradiation of the samples does not affect the kinetic parameters of the dissolution such as the partial order relative to the proton concentration in acidic media ($n = 0.37 \pm 0.01$ and $n = 0.34 \pm 0.01$ for unirradiated and fully amorphized β-TUPD samples, respectively) or the activation energy of the reaction of dissolution ($E_{app} = 49 \pm 4$ kJ mol^{-1} and 42 ± 4 kJ mol^{-1} for unirradiated and partly amorphized samples with $f_A < 1$, respectively).

This paper focuses on the thermodynamic approach of the pre-irradiation influence on the dissolution, with the observation and the characterization of neoformed phases potentially formed onto the surface of the leached pellets. As a comparison, the same study was already performed on unirradiated samples [8].

2. Experimental

2.1. Samples preparation

β-TUPD samples were prepared by wet chemistry processes, through the precipitation of thorium–uranium (IV) phosphate hydrogenphosphate hydrate (TUPHPH): $U_{0.2}Th_{1.8}(PO_4)_2(HPO_4)\cdot H_2O$, as a crystallized low-temperature precursor [9]. This precipitation step occurs from a mixture of thorium nitrate or chloride solution (0.7 M) and 5 M phosphoric acid in the mole ratio $Th/PO_4 = 2/3$. The gel initially formed is slowly transformed into the well crystallized TUPHPH by heating at 433 K on a sand bath for several hours. β-TUPD sintered pellets are obtained after pressing the resulting powder (room temperature, 200 MPa) then heating at 1523 K for 10 h in alumina boats under inert atmosphere (Ar). Samples were characterized by Electron Probe MicroAnalyses (EPMA) to check the homogeneity, the purity and the elementary composition of the sintered samples before irradiation.

2.2. Irradiation experiments

The structural stability of the ceramic under irradiation was first studied using high-energy heavy-ions which interact with the material mainly through excitation and ionization (electronic energy loss) except at the end of the path of ions where the nuclear contribution predominates. Such experiments enable to study the influence of the electronic energy loss. The irradiation experiments were performed on the SME line at GANIL (Caen, France) using 840 MeV Kr ion beam. The projected range R_P and the range straggling ΔR_P were estimated to $R_P = 72$ μm and $\Delta R_P = 0.79$ μm for 840 MeV Kr from the SRIM code [10]. Each irradiated sample was finally characterized through XRD experiments to determine the amorphous fraction associated to each irradiation fluence (Table 1).

2.3. Leaching tests

The leaching tests were performed in HNO_3 in static conditions (without any significant renewal of the leachate). High-density polyethylene containers and PTFE vessels were used for the experiments at room temperature and above 343 K, respectively. The concentrations of cations were determined by Inductively Coupled Plasma-Mass Spectroscopy (ICP-MS) for Th and U and by Time Resolved Laser Induced Fluorescence Spectroscopy (TRL-IFS) for U [6]. The normalized dissolution rate R_L (g m^{-2} d^{-1}) which represents the mass loss of solid per time and surface units, was calculated from the following equation:

Table 1
Amorphous fraction f_A of β-TUPD corresponding to the irradiation fluence (840 MeV Kr)

Fluence (cm^{-2})	No irradiation	5×10^{11}	10^{12}	2×10^{12}	3×10^{12}	10^{13}
Amorphous fraction f_A (–)	0	0.2	0.4	0.6	0.8	1

$$R_L(i) = \frac{dN_L(i)}{dt} = \frac{d}{dt}\left(\frac{C_i \times V \times M_i}{x_i \times S}\right), \quad (1)$$

where C_i represents the concentration of the measured element (Th, U), V the volume of the leachate, x_i the mass ratio of the element i in the solid, M_i the molar mass of i and S the effective surface area of the pellet. Leaching tests were driven in HNO_3 with various conditions of pH and temperature.

3. Results and discussion

3.1. Behaviour of actinides during the dissolution

From the obtained data, both actinides exhibit different behaviours during dissolution: uranium (IV) is released in the solution (consequently to its oxidation into uranyl) while thorium is precipitated in a phosphate-based neoformed phase. Previous studies have revealed that this quantitative precipitation occurs more quickly for high temperature or pH values (pH > 1) leading to an incongruent dissolution (*i.e.*, $r = R_L(U)/R_L(Th) > 5$) [11]. For pH = 1, thorium is released in the leachate with the same normalized dissolution rate than uranium (congruent dissolution: $r = 1$) then precipitates for longer leaching times.

The same results were obtained in the case of leaching of pre-irradiated samples. However the congruent step of dissolution is strongly influenced by the pre-irradiation, the transition between congruent and incongruent phases occurring more quickly for high-amorphous fraction f_A (Fig. 1). Whatever the leaching conditions, this incongruent dissolution step (*i.e.*, pH > 1 and high-temperature) is bound to the increase of the normalized leaching with f_A which enables to reach more quickly the saturation conditions of the leachate. Consequently, for pre-irradiated samples, the precipitation occurs after a shorter leaching time.

Whatever the experimental conditions (T, pH, f_A, etc.), the formation of the neoformed phases onto the surface of the leached sample is correlated to a plateau in the N_L(Th) variation (due to saturation conditions) and to a slowing down of the associated normalized dissolution rate R_L(U) (Figs. 1 and 2(a)). This observation results from the formation of a neoformed layer onto the surface which leads

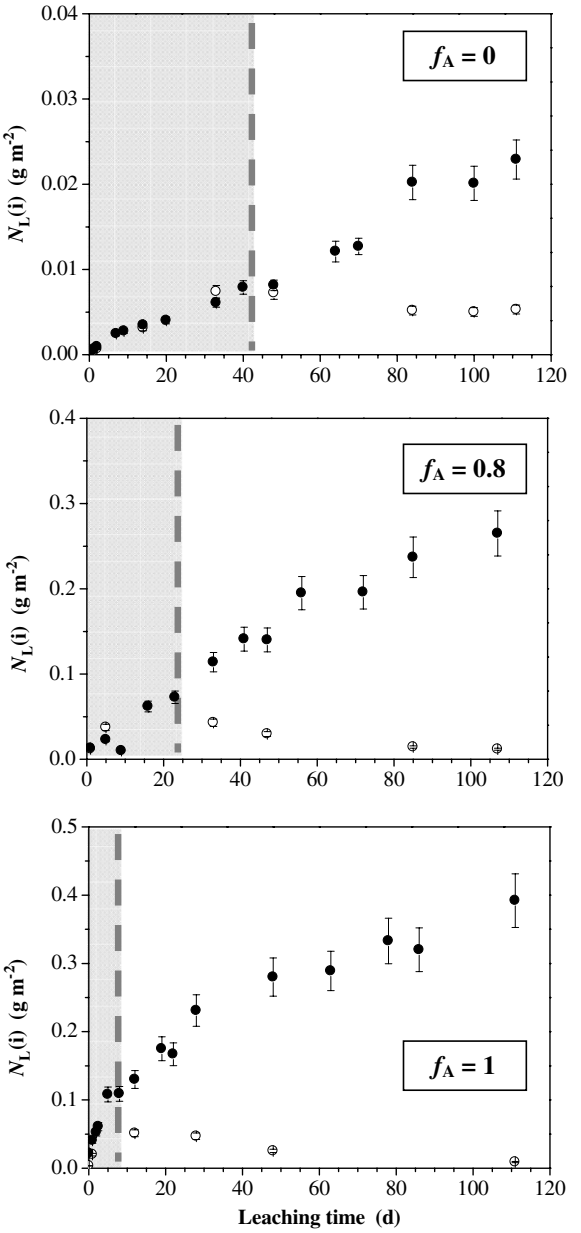

Fig. 1. Evolution of the normalized leachings N_L(Th) (○) and N_L(U) (●) during the leaching of unirradiated and pre-irradiated samples with different amorphous fractions (10^{-1} M HNO_3, $T = 363$ K). The tinted zones correspond to the congruent of the dissolution.

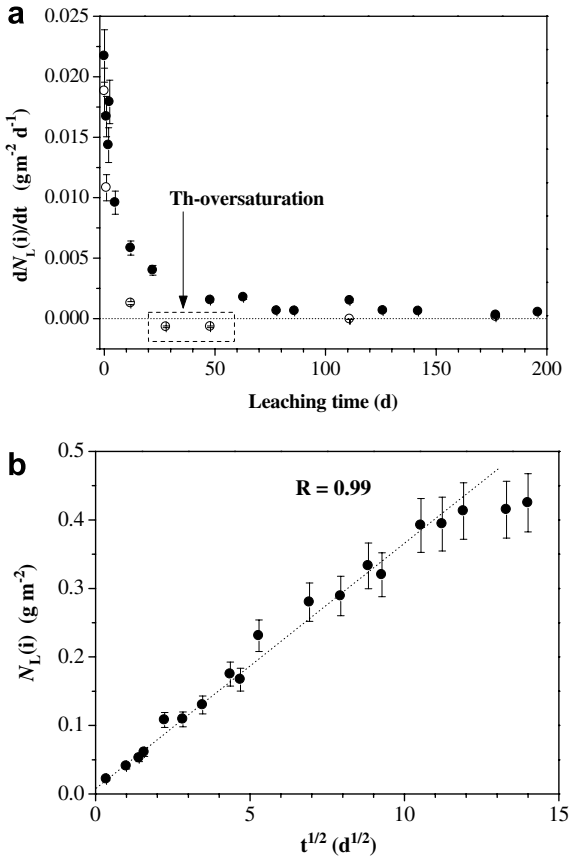

Fig. 2. Evolution of the normalized dissolution rate R_L(Th) (○) and R_L(U) (●) (a) and variation of the normalized leachings N_L(Th) (○) and N_L(U) (●) versus the square root of the leaching time showing diffusion phenomena (b) (10^{-1} M HNO_3, $T = 363$ K).

to a diffusion regime driving the release of ions from the solid to the leachate. The linear variation between the square root of the leaching time and the normalized leaching, N_L(U), confirms such diffusion phenomena (Fig. 2(b)). The slight gap between the slope and the experimental data for important leaching times is due to the precipitation of uranium (VI) as the uranyl phosphate pentahydrate $(UO_2)_3(PO_4)_2 \cdot 5H_2O$ [6]. The observed slowing down of the release of actinides from the solid to the leachate clearly illustrates the protective role on the neoformed phase and justifies its identification and its complete characterization.

3.2. Precipitation of neoformed phase(s)

In order to evidence the neoformed phases onto the solid when saturation conditions are reached in the leachate, Scanning Electron Microscopy (SEM) observations were driven on pre-irradiated (840 MeV Kr ion beam) then leached (10^{-1} M HNO_3) β-TUPD samples for several amorphous fractions. Whatever the f_A value, they revealed an important modification of the surface of the material in three steps, observable in Fig. 3.

The alteration first occurs preferentially inside the grain boundaries (Fig. 3(a)) and leads to the break away of the grains. This step is followed by the formation of a gelatinous layer, probably amorphous, which 'spiderwebs' appearance may be due to the drying under vacuum (Fig. 3(b) and (c)). This phase is unstable under vacuum or electronic beam, which made impossible its extensive characterization by SEM and EPMA. A crystallized phase is also observed: it appears as circular plates of 2–8 μm (Fig. 3(a)–(c)) or as bigger aggregates looking like 'cockscombs'. This morphology is similar to that of thorium phosphate–hydrogen phosphate hydrate (TPHPH), $Th_2(PO_4)_2(HPO_4) \cdot H_2O$. For longer leaching times, the crystallized phase recovers the whole surface of the sample (Fig. 3(d) and (e)) thus acts as a protective layer for raw material. Backscattering Electron observation evidences that the neoformed phase also precipitates inside the cracks of the solid.

These different steps, observed for every amorphous fractions, were already described in the case of unirradiated β-TUPD samples [8]. It confirms the unimportance of the pre-irradiation on the precipitation process, expected for the delay required to reach the saturation conditions.

3.3. Characterization of the neoformed phase

The identification of the neoformed phase as TPHPH, deduced from SEM observations and previous studies, was confirmed by complementary experiments realized on the neoformed phase.

Elementary compositions of the solid bulk and of the neoformed phase onto the surface of the leached pellets were determined by EPMA experiments and compared to that of the solid precipitated in over saturation conditions, corresponding to TPHPH (Table 2). These results evidence the uranium depletion in the neoformed phase (①) by comparison to the bulk material (②), confirming the quantitative thorium-precipitation in the phosphate-based phase and the release of uranium in the leachate. Furthermore, the mole ratio (U + Th)/P of 0.70 is in good agreement with those of β-TPD and TPHPH.

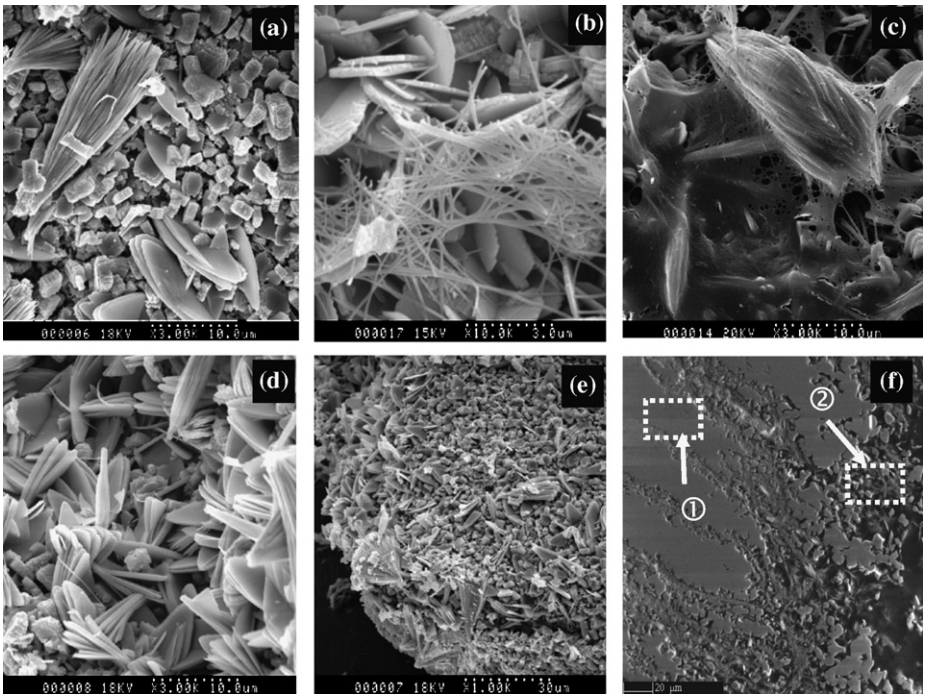

Fig. 3. SEM observations of pre-irradiated leached β-TUPD (10^{-1} M HNO_3, $T = 363$ K) for $t = 350$ days (a), $t = 450$ days (b), (c) and $t = 800$ days (d), (e). Associated backscattering electron micrograph of a crack, $t = 800$ days (f).

Table 2
EPMA results obtained for pre-irradiated then leached β-TUPD pellet (840 MeV Kr, fluence: 10^{13} cm^{-2}, $f_A = 1$; 10^{-1} M HNO_3, $T = 363$ K, $t = 800$ d)

	Bulk (①)	Neoformed phase (②)	TPHPH
U (wt%)	5.1 ± 0.5	0.3 ± 0.2	0
Th (wt%)	57.2 ± 0.7	62.2 ± 1.3	60.3 ± 0.5
P (wt%)	12.5 ± 0.3	12.1 ± 0.7	12.5 ± 0.5
Mole ratio (–) U/(Th + U)	0.08 ± 0.01	<0.05	0
Mole ratio (–) (U + Th) / P	0.66 ± 0.02	0.70 ± 0.07	0.66

The μ-Raman spectrum, recorded on the surface of the leached β-TUPD, exhibits all the vibration bands characteristic of TPHPH (Fig. 4(a)). The P–O bond of the PO_4 groups can be assigned considering the data reported in the literature [12]: δ_s (372–428 cm^{-1}), δ_{as} (574–619 cm^{-1}), ν_s (990 cm^{-1}) and ν_{as} (1023–1150 cm^{-1}). Moreover, the binding vibration band of the P–O–(H) group located at 912 cm^{-1} confirms the presence of HPO_4 groups [13]. XRD spectra were also recorded on the isolated neoformed phase. For μ-Raman and XRD analyses, the comparison with the reference spectra of TPHPH confirms the nature of the neoformed phase. Thus, the precipitation corresponds to the following equilibrium:

$$Th_2(PO_4)_2(HPO_4) \cdot H_2O \leftrightarrows Th^{4+} + 2PO_4^{3-} + HPO_4^{2-} + H_2O \quad (2)$$

with the associated solubility constant:

$$K^{\circ}_{S,0} = [Th^{4+}]^2 [PO_4^{3-}]^2 [HPO_4^{2-}] \times (\gamma_{Th^{4+}})^2 \left(\gamma_{PO_4^{3-}}\right)^2 \left(\gamma_{HPO_4^{2-}}\right). \quad (3)$$

From the elementary concentrations determined in the leachate, the constant value was calculated for different amorphous fractions of the pre-irradiated leached solids. It appears that the amorphous fraction has no influence on the solubility constant value (Table 3) which average was estimated to $10^{-70.6 \pm 1.3}$ at $T = 363$ K and $10^{-67.7 \pm 1.7}$ at $T = 298$ K. It also enables to follow the evolution of the free enthalpy of reaction (2) (Fig. 5), which evidences the distance to the thermodynamic equilibrium:

$$\Delta_R G = RT \ln \left(\frac{Q_S}{K_S}\right). \quad (4)$$

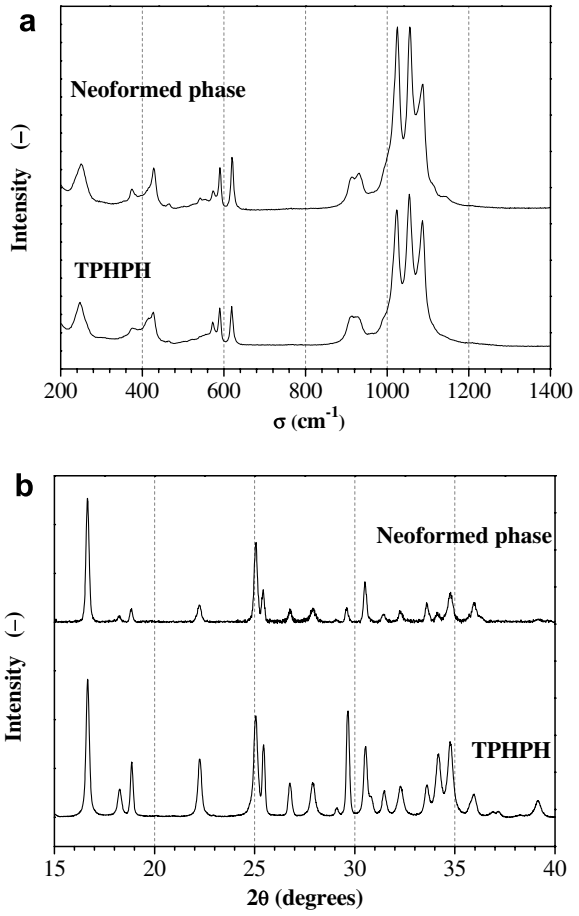

Fig. 4. μ-Raman spectra (a) and XRD diagrams (b) of TPHPH and of the neoformed phase collected at the surface of pre-irradiated leached β-TUPD (10^{-1} M HNO_3, $T = 363$ K, $t = 800$ days).

Table 3
Solubility product of TPHPH determined in the case of leaching of pre-irradiated samples of different f_A

Medium	f_A (–)	$T = 363$ K	$T = 298$ K
10^{-1}M HNO_3	0	−72.3	−68.7
10^{-4}M HNO_3			−64.6
10^{-1}M HNO_3	0.2	−69.1	
10^{-4}M HNO_3			−68.5
10^{-1}M HNO_3	0.4	−70.3	
10^{-1}M HNO_3	0.8	−71.7	
10^{-4}M HNO_3			−68.2
10^{-1}M HNO_3	1	−69.9	−68.4
10^{-4}M HNO_3			−64.7
Average value		-70.6 ± 1.3	-67.7 ± 1.7

The $\Delta_R G$ value is negative at the beginning of the leaching test (*i.e.*, far from thermodynamic equilibrium) showing the absence of precipitation. Then, it tends quickly to zero through oscillations when the equilibrium conditions are reached. Moreover, the comparison between the $\Delta_R G$ evolution for fully amorphized and unirradiated samples confirms that the saturation occurs more rapidly for high-amorphous fraction.

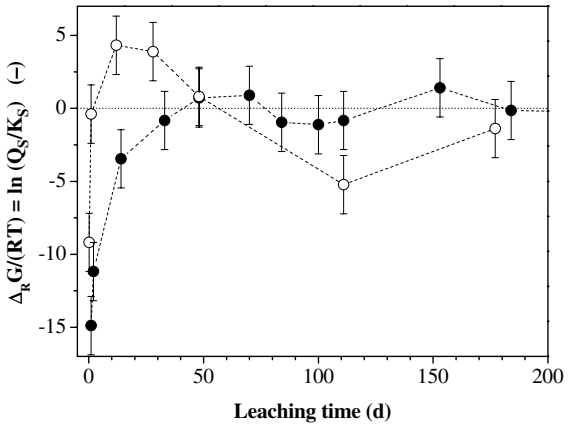

Fig. 5. Evolution of $\Delta_R G/RT$ associated to the TPHPH dissolution during the leaching tests of unirradiated (●) and amorphized (○) β-TUPD samples.

4. Conclusion

This study has evidenced the influence of the pre-irradiation on the thermodynamic aspect of the β-TUPD dissolution. The only significant effect lies in the required delay to reach the incongruent step, saturation conditions occurring more rapidly for high-amorphous fraction, consequently to the increase of the normalized dissolution rates. However, the precipitation processes are similar to those described in the case of unirradiated samples: thorium precipitates in phosphate-based phase while uranium is released in solution thanks to its oxidation into the uranyl form. This neoformed phase was identified as TPHPH thanks to SEM observations, EPMA, XRD and μ-Raman experiments. Its formation provides a protective layer onto the surface of the leached solid by limiting the release of actinides. As the saturation conditions are reached more rapidly for pre-irradiated samples, this protective action occurs earlier. In these conditions, the increase of the normalized leaching due to pre-irradiation is counterbalanced by the more rapid formation of protective layer.

Acknowledgements

This work was financially supported by the french research program NOMADE (GDR 2023 CNRS/CEA/COGEMA). The authors are grateful to R. Podor, J. Ravaux and A. Kolher from LCSM of Nancy (France) for making the EPMA analyses and the SEM observations. They also want to thank T. Lhomme from CREGU (University Henri Poincaré of Nancy, France) for performing the μ-Raman experiments.

References

[1] N. Dacheux, A.C. Thomas, V. Brandel, M. Genet, J. Nucl. Mater. 257 (1998) 108.
[2] N. Dacheux, R. Podor, V. Brandel, M. Genet, J. Nucl. Mater. 252 (1998) 179.
[3] N. Dacheux, A.C. Thomas, B. Chassigneux, E. Pichot, V. Brandel, M. Genet, Mater. Res. Soc. Proc. 556 (1999) 85.
[4] B.D. Begg, N.J. Hess, W.J. Weber, R. Devanathan, J.P. Icenhower, S. Thevuthasan, B.P. McGrail, J. Nucl. Mater. 288 (2001) 208.
[5] C. Tamain, F. Garrido, L. Thomé, N. Dacheux, A. Özgümüs, A. Benyagoub, J. Nucl. Mater. 357 (2006) 206.
[6] A.C. Thomas, N. Dacheux, P. Le Coustumer, V. Brandel, M. Genet, J. Nucl. Mater. 295 (2001) 249.
[7] C. Tamain, N. Dacheux, F. Garrido, A. Habert, N. Barré, A. Özgümüs, L. Thomé, J. Nucl. Mater. 358 (2006) 190.
[8] N. Clavier, E. du Fou de Kerdaniel, N. Dacheux, P. Le Coustumer, R. Drot, J. Ravaux, E. Simoni, J. Nucl. Mater. 349 (2006) 304.
[9] N. Clavier, N. Dacheux, P. Martinez, V. Brandel, R. Podor, P. Le Coustumer, J. Nucl. Mater. 335 (2004) 397.
[10] J.F. Ziegler, J.P. Biersack, U. Littmark, in: J.F. Ziegler (Ed.), The Stopping and range of ions in solids, Vol. 1, Pergamon, New York, 1985.
[11] N. Dacheux, N. Clavier, J. Ritt, J. Nucl. Mater. 349 (2006) 291.
[12] N. Dacheux, N. Clavier, G. Wallez, V. Brandel, J. Emery, M. Quarton, M. Genet, Mater. Res. Bull. 40 (2005) 2225.
[13] M. Trchova, P. Capkova, P. Matejka, K. Melanova, L. Benes, J. Solid State Chem. 145 (1999) 1.